

Erosion And Deposition Comparison Of Biochar, Pumice, And Arizona Test Dust On Titanium Coupons

Menwa Besheer¹, Kristin Eickelbeck², Kiara Kulkarni³, Chris Morgan⁴,
Katherine Tyler⁵

Virginia Tech, Blacksburg, VA 24060, United States

A study was conducted to determine the different behavior between sand, volcanic ash, and wildfire ash when ingested by an aircraft engine, with a focus on erosion and deposition. In the field of ingestion research, sand and volcanic ash have been studied numerous times, but no studies have been conducted on wildfire ash. As wildfires become more prevalent and dangerous, it is important to begin to characterize the damage wildfire ash particles can cause as aircrafts fly through ash clouds. Arizona Test Dust (ATD) was used to simulate sand, pumice for volcanic ash, and biochar for wildfire ash. A comparison was made to both validate the testing procedure and set up as well as determine where the biochar fit with well-known particulates. Preliminary testing suggested improvements to the testing procedure were needed to eliminate large particles and clogging of the injector. These preliminary tests also showed interesting results of deposition with biochar which was further investigated in this study. To address the concerns that were presented during the preliminary testing, the particulates were milled down then separated into to the desired size range of 50-150 microns using a sieve shaker. Additionally, the rig was modified to better accommodate biochar. Then, the particulates were fed into a free jet at 9 g/min flowing at Mach 0.65 before impacting a titanium coupon, used to simulate a compressor blade. The surface roughness of each coupon was measured before and after testing to characterize the erosion and deposition caused by each particulate. A visual inspection was conducted on each coupon before and after testing using a 3D profilometer. The surface roughness showed the largest increase on coupons exposed to ATD, then pumice and finally biochar. These results indicate that ATD is the most erosive, then pumice, and biochar causes the least erosion. The visual inspection confirmed these results and showed the greatest deposition with biochar. There was some deposition with ATD and little to no deposition with pumice. Overall, this study validated the testing procedure and rig, especially for the use of biochar allowing for future studies to use this rig and further explore the deposition caused by biochar. This study indicates that aircraft with prolonged exposure to wildfire ash should have additional inspections completed to check for harmful deposition.

I. Introduction

Wildfire ash ingestion in aircraft engines is a rising problem with the increase in the number and severity of wildfires. Since 2013, an average of 7.2 million acres of land have been burned by wildfires each year [1]. Wildfire ash can travel long distances and stay in the air for weeks due to its miniscule size and the powerful upward forces created by intense heat during wildfires [2]. These small ash particles easily get carried by winds that can transport

¹ Undergraduate student, Aerospace & Ocean Engineering Department, AIAA Student Member (1373963)

² Undergraduate student, Aerospace & Ocean Engineering Department, AIAA Student Member (1601401)

³ Undergraduate student, Aerospace & Ocean Engineering Department, AIAA Student Member (1602923)

⁴ Undergraduate student, Mechanical Engineering Department, AIAA Student Member (1810529)

⁵ Undergraduate student, Mechanical Engineering Department, AIAA Student Member (1810532)

them over vast areas. As aircraft fly in proximity to wildfires, engines components are exposed to ash dense conditions that have potential to damage engines [3]. Due to the prolonged suspension of wildfire ash in the atmosphere, aircraft engines used in various other sectors, such as commercial aviation, can also contact ash particles. This is an important consideration as it emphasizes the need for understanding and mitigating the effects of wildfire ash ingestion on engines and aircraft operations.

While research has been previously conducted to investigate the effects of sand and volcanic ash ingestion [4], not enough work has been done to understand the effects of wildfire ash ingestion. The objective of this research is to fill that gap and see how the effects of wildfire ash compare to sand and volcanic ash, specifically looking at the erosion and deposition rate and how it compares between each particulate. Since this is a new area of study, it can help the aviation industry with ingestion testing with their current engines and improving the future engines to overcome the presented problem [5].

The VIPR III (Vehicle Integrated Propulsion Research) project conducted a testing program using a commercial engine to simulate volcanic ash ingestion, using pumice as a substitute [6]. Key findings included notable damage to compressor blades and vanes, with observations of "tip distress" and "blade roughness and rounding" after a full engine breakdown. Microscopic analysis revealed that the jagged shapes and large diameters of volcanic ash closely resemble those of wildfire ash. The study drew comparisons between the two types of ash which involved techniques that provided high-resolution images of particle morphology and size distribution, suggesting that similar conclusions could be drawn from experiments involving wildfire ash.

In parallel, research by Dr. Wing F. Ng at Virginia Tech focused on the effects of sand sticking to heated coupons [7]. Results indicated that factors such as flow rate, pressure ratio, sand amount, average sand diameter, flow area, and metal temperature influenced blockage. The study proposed future work involving different forms of sand for varied results.

To compare the effects of wildfire ash to the previously studied volcanic ash and sand, a preliminary test was conducted to create an erosion scale for the three particulates. Biochar was used to simulate wildfire ash, Arizona Test Dust was used to simulate sand, and pumice was used for volcanic ash. The heated free jet at the Advanced Propulsion and Power Laboratory (APPL) at Virginia Tech was used to propel the particulates at titanium coupons that simulated a compressor blade in an engine. After each coupon was exposed to the particulate, the erosion and deposition were measured. Deposition was seen during this preliminary testing conducted by the Wildfire Ash Ingestion Team during Spring 2023, so it was predicted that deposition would be seen again. However, many issues were seen with the preliminary testing resulting in high levels of uncertainty. The injector system clogged to the point where pumice was unable to be tested, and the flow rate of the biochar was cut in half. The goals of this study are to build on the work conducted in Spring 2023 by eliminating the areas of uncertainty and working to quantify deposition since the preliminary tests confirmed that biochar led to deposition.

II. Apparatus and Techniques

A. Particulates and coupons

Three different particulates were tested in this experiment to simulate sand, volcanic ash, and wildfire ash. First, Arizona Test Dust (ATD) was used to demonstrate sand. The Arizona Test Dust was obtained from Powder Technology Inc. with PTI ID: 15164C and model identification name ISO 12103-1, A4 Coarse Test Dust. Second, pumice was used to represent volcanic ash. The pumice was purchased from General Pumice Products at a size of 0.125". Third, biochar was used to simulate wildfire ash. The biochar was produced by the manufacturer Soil Reef through a process called pyrolysis, which is the process of biomass being burned without combustion.

Grade 5, 6Al-4V titanium coupons were used in this study to represent the compressor blades in an engine. This titanium was selected because it is comparable to the metal of uncoated aircraft compressor blades. The titanium was purchased from the Performance Titanium Group and manufactured into 2" x 1" coupons. The coupons had been used in previous testing, so they were polished with 3000 grit sandpaper to a near mirror finish and cleaned with an ultrasonic cleaner. Three of the coupons, one to be used for each particulate, were coated with blue layout fluid to visualize the particulate impact on the coupon and confirm particles were contacting the coupon. This was proven to be a successful visualization technique in the preliminary testing. The ink used was Dykem 80300 Steel Blue Layout Fluid.

B. Instruments

The pumice and biochar were milled using a long roll jar mill from US stoneware (model 801CVM, serial number CM06001). The ATD was not milled as it already met the desired size range. The jar mill has 36 inch long rollers and runs from a 5 horsepower motor [8]. The particulate matter was put into the jar with various sized ceramic balls to grind the particulate down to the desired size. The jar was placed on the rollers then allowed to roll for approximately 1 hour and 30 minutes. After the particulate was milled, it was put through a W.S. Tyler Ro-Tap Model E Test Sieve Shaker to filter the particulate to the desired size range of 50 microns with a maximum of 150 microns. The shaker consisted of 3 filters, from the Fisher Scientific Company, with openings of 1.70 mm, 150 microns, and 45 microns, stacked in that order. The particulate caught by the 45 micron sieve was used for the experiment. The particulate filtered in the sieve can be seen in Figure 1.

To verify that the milling and sieving process produced particles of the desired size, the size distribution of each particulate was taken using a Horiba Partica LA-950 laser scattering particle size distribution analyzer. The size distributions of the particulate are shown below in Figure , Figure , and Figure . The LA-950 has a precision of +/- 0.1% accuracy of +/- 0.6% [9].



Figure 1. Pumice after shaking sieve

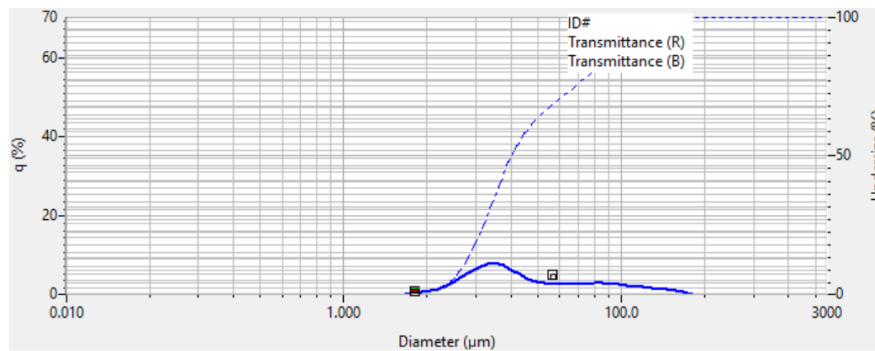


Figure 2. Biochar particle size distribution

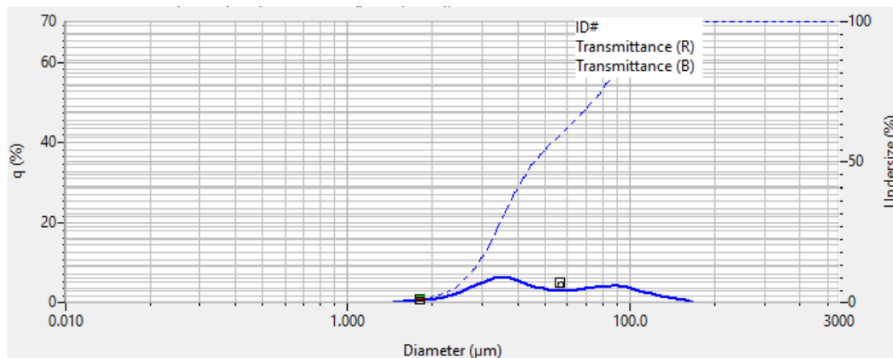


Figure 3. Pumice particle size distribution

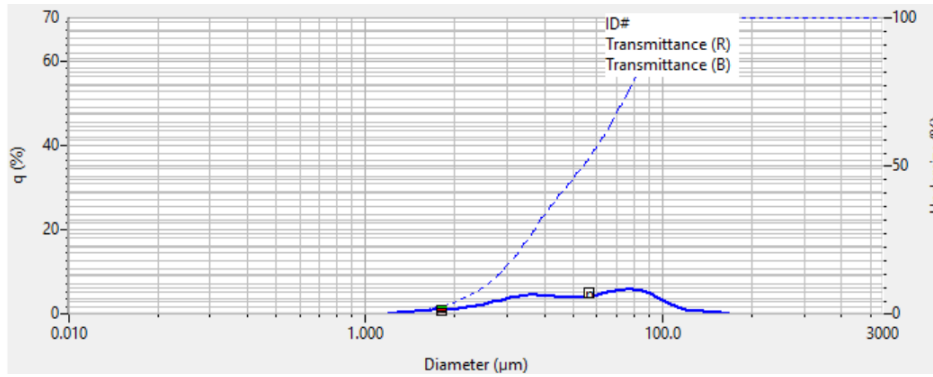


Figure 4. Arizona Test Dust particle size distribution

As seen in the size distributions above, the particle refinement process worked well to achieve the desired particulate size. The particle size distributions are similar for each particulate which allows for better comparison. The mean sizes of the particulate are seen in **Error! Reference source not found.** While all the particulate mean sizes were below 50 microns, the desired size, this size is ideal as it lowers the chances of the particulate clogging the injector system.

The surface roughness of the coupons was taken at several points during testing to quantify erosion on the coupons. The surface roughness

Table 1. Particulate size averages

Particulate	Mean Size (µm)	Geometric Mean Size (µm)
Biochar	38.9336	21.8881
Pumice	21.1631	28.4844
Arizona Test Dust	29.1218	27.0370

gauge used was the Mitutoyo SJ-210. The SJ-210 has a range of 1,000 microinches with a resolution of 0.08 microinches [10]. To gain additional insight into the surface of the coupons, they were examined using a Keyence VK- X3000 3D profilometer, which provides up to 28,800 times magnification. It has a resolution of 0.01 nanometer across a 50 millimeter by 50 millimeter area [11]. The mass of the coupon was also taken at several points during the experiment, using the A-200DS scale from Dever Instrument Company. The scale has a readability of 0.1 mg and a capacity of 200 grams [12].

C. Free Jet and injector system

Particulate was injected into the heated free jet at the APPL to achieve velocities seen in engines in operating conditions. To load the particulate into the injector system, the particulate was spread evenly on a conveyor belt system. When the belt advances, the particulate drops onto a funnel which connects to the injector system. The speed of the belt determines the duration of the test. The mass of particulate placed on the belt divided by the time it takes for the back of the belt to reach the front determines the mass flow rate of particulate. The maximum duration of a run is 2 minutes due to the limits of the motor and control system. A venturi device creates suction which propels the particulate into the flow of the free jet. The flow passes through a converging nozzle then an extension tube, resulting in the particulate reaching near flow velocity. The flow exits the extension and collides with the surface of the coupon. The coupon is oriented normal to the flow as shown in Figure 5.

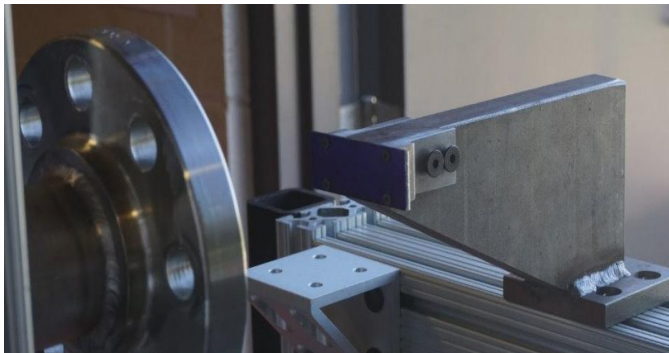


Figure 5. Coupon set up in front of the jet

In previous experiments conducted by the team, an injector containing a series of drilled holes was used to uniformly distribute the particulate in the flow. The model of the old injector is shown in Figure 6. However, several occurrences of clogging and flow reversal during injection lead to a new system to be developed and utilized. In place of the series of small exit openings, the tube carrying the particulate was bent toward the direction of flow allowing particulate to directly enter the stream with no obstruction. The new model is shown in Figure 7. The single large opening prevents clogging and allows for greater mass flow rates. Even distribution

of particulate in the flow was validated using the coupons painted with layout fluid to visualize the particle coupon interaction. When tested with ATD, pumice, and biochar, no significant difference was observed between the new and old injectors in terms of particulate distribution. In previous experiments, biochar with a mass flowrate of 9 grams per minute or greater was observed to rapidly clog the old injector. The mass flow rate was reduced to 4.5 grams per minute to reduce clogging. The new injector system underwent a series of tests with varying flowrates of biochar, the particulate most prone to clogging. The new system succeeded with flowrates of 9 grams per minute, 13.5 grams per minute, and 18 grams per minute and were tested for a duration of 2 minutes. No sign of partial flow reversal or clogging was observed, therefore the system may be able to handle an excess of 18 grams per minute, though future testing is needed for verification. If clogging occurs the injector system must be removed from the free jet and disassembled, which delays further testing and increases wear on components.



Figure 6. Side view of old injector system



Figure 7. Side view of new injector system

D. Procedure and Parameters

Before testing, the particulate was refined to ~50 micron. The pumice and biochar were milled until a fine powder was obtained. The milled pumice and biochar as well as the ATD were then transferred to a sieve shaker. Particulate sized less than 50 microns and greater than 150 microns were eliminated.

The titanium coupons were polished using sandpaper starting at 120 grit and ending at 3000 grit to achieve consistent surfaces that represent those of a compressor blade. The coupons were placed in an ultrasonic cleaning bath to remove residue from polishing. Surface roughness measurement and 3D Profilometer scans were performed at the center of each coupon. Mass measurements of each coupon were conducted. Three out of the thirteen coupons were painted with layout fluid, one to test with each type of particulate. One coupon was reserved for testing with only air, and 3 coupons were reserved for exposure to each type of particulate.

For each test, 18 grams of each particulate were spread evenly across the conveyer belt. The belt speed was set to 2 minutes per run, achieving a mass flow rate of 9 grams per minute. Testing one coupon per run, coupons were loaded on to the mount, the free jet was set to a flow velocity of Mach 0.65. After each run, the coupons were removed from the mount and carefully placed in individual containers. After testing, surface roughness and mass measurement were recorded. The surface was scanned with a 3D profilometer. The coupons were then cleaned with an ultrasonic cleaner to remove all deposited particulate, and the mass and surface roughness measurements were taken again.

III. Results and Discussion

A. Surface Roughness

The surface roughness of the titanium coupons was measured before and after exposure to the particulate, and again after the coupons were cleaned using ultrasonic cleaning. The purpose of measuring the surface roughness was to quantify the erosion caused by each of the three particulates. The average surface roughness for each particulate is shown in Table 2 below. The roughness of the coupons significantly increased after exposure to all three particulates.

Table 2. Comparing the average surface roughness of the 3 particulates at different stages of testing Procedure

Particulate	Average Initial Surface Roughness [μin]	Average Surface Roughness After Exposure [μin]	Average Surface Roughness After Cleaning [μin]
Arizona Test Dust	4.605	30.7625	33.1075
Pumice	5.2525	26.825	25.175
Biochar	5.3767	13.2133	8.83

The change in surface roughness before and after exposure to the particulate was calculated for each coupon and plotted in Figure 8. The figure also includes dashed lines to represent the average change in roughness for each particulate. ATD caused the greatest change in surface roughness at approximately 26 micro inches. Followed by pumice with a surface roughness change of 21.5 micro inches. Then, biochar with difference of about 8 micro inches. This indicates that ATD is the most erosive and biochar is the least erosive.

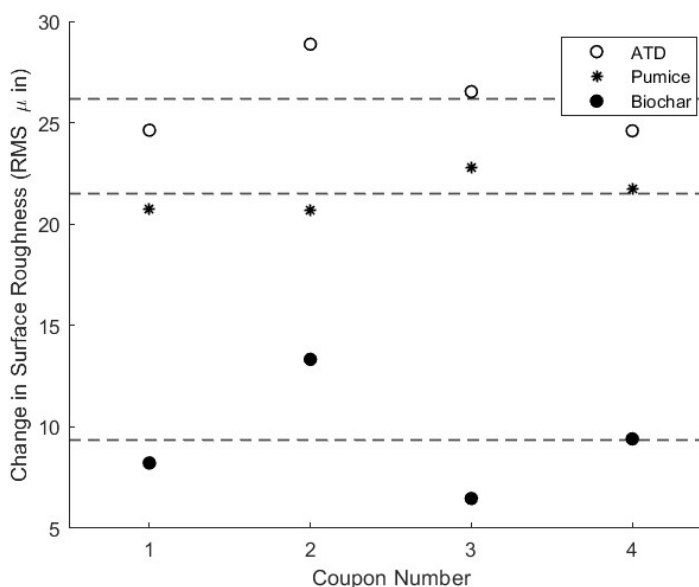


Figure 8. Comparison of the change in surface roughness for the three particulates

Following the cleaning procedure, the coupons exposed to ATD demonstrated an increase in surface roughness, whereas those treated with pumice and biochar exhibited a decrease in surface roughness. The change in surface roughness in the ATD coupons is about 2.3 μin . Pumice had the smallest change of 1.65 μin . Biochar exhibited the highest change after cleaning as the surface roughness went down by 4.38 μin . The change in the surface roughness measurement for the coupons exposed to biochar could be a result of the elimination of the deposition from using ultrasonic cleaning. The biochar that got stuck to the coupon could have caused bumps which increased the surface roughness. After cleaning the coupons, the particulates were removed resulting in a slightly smoother surface.

B. Mass

The mass of each coupon was measured before testing, after the test was performed, and after the coupons were cleaned. The goal of weighing the coupons was to quantify the amount of particulates that stuck to coupons as well as the amount of material that was eroded. The difference between the second and third measurement was supposed to indicate the amount of particulate that accumulated on the coupons while the difference between the first and last measurement was supposed to quantify the amount of material that eroded. The average mass of the coupons for each measurement is provided in Table 3.

The inconsistency of the mass measurements is most likely due to the insignificant changes in the mass after each step of the procedure. The scale used in this study was not precise enough to capture those minor changes. The mass data has been

Table 3. Comparing the average mass of the coupons exposed to the 3 different particulates at different stages of testing

Particulate	Average Initial Mass[g]	Average Mass After Exposure [g]	Average Mass After Cleaning [g]
Arizona Test Dust	23.90235	23.901525	23.9047
Pumice	24.870475	23.8775	23.891475
Biochar	23.75031667	23.79304	23.7996

considered inconclusive for this study. It is suggested to utilize another method to quantify deposition in future studies. One proposed idea is to use an electron microprobe analyzer (EMPA) to scan the surface of the coupon and detect titanium (the coupon) versus the particulate (e.g. carbon for biochar). This would allow for a determination of what percentage of the coupon the particulate is covering.

C. Visual Inspection

The surfaces of the coupons were inspected using a 3D Surface profilometer. The surface of each coupon was scanned before and after the test was performed to identify the changes to the surface of the coupon, specifically identifying spots of erosion and deposition. Figure 9 shows the initial surface of a coupon under 2.5x magnification. This image was taken at the center of the coupon. The small scratches covering the surface of the coupon are a result of polishing the coupon with sandpaper. Overall, the surface of the coupon is relatively smooth, and there are no noticeable indents or bumps.

Figure 10 shows the optical view of a coupon exposed to ATD under 2.5x magnification, and Figure 11 shows the 3D view of the same coupon under the same magnification.



Figure 10. Optical view of coupon exposed to ATD at 2.5x

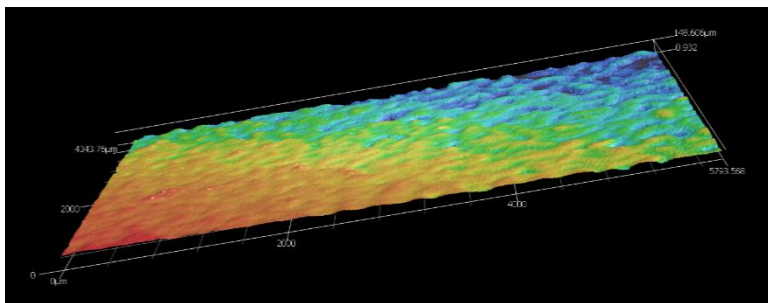


Figure 11. 3D scan of coupon exposed to ATD at 2.5x magnification

Similar to the results from the ATD coupons, the coupons exposed to pumice showed no signs of the initial scratches. This indicates that the pumice was eroding the surface of the coupon, despite the smooth looking surface in the optical view. However, in comparison to the ATD, the surface of the coupon exposed to pumice was not as rough. Little to no deposition was found from the visual inspection that was conducted. These results suggest that in the colder sections of the engine, such as the compressor, volcanic ash will not cause serious deposition, but it has the potential to erode the compressor blades. Literature suggests that particulates ingested by an engine can first smooth compressor blades and lead to greater efficiency, but

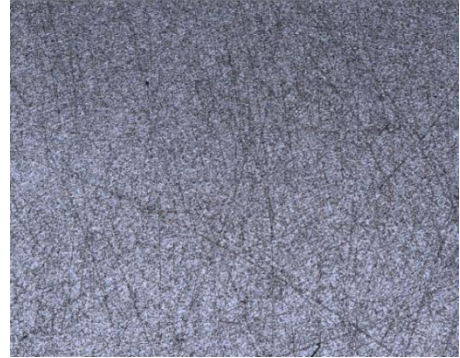


Figure 9. Initial image of a coupon under 2.5x magnification

These images show visual evidence of erosion from the ATD particles.

While the coupon appears smoother in the optical image (Fig. 10), the scratches that covered the coupons initially have been eroded away by the ATD. The surface of the coupon is rough and shows signs of pitting in some spots as can be seen by the 3D scan. These results are consistent with the preliminary testing carried out in 2023, and other sand ingestion experimentation. These images also confirm the results from the surface roughness tests. Furthermore, there were also a few spots of deposition found where a grain of ATD stuck to the coupon. However, deposits left by the Arizona Test Dust were not common as only a few particulates stuck to the coupon were found. Erosion was found to be the larger result as seen by the pitting, erosion of the scratches, and the rough surface. These results

indicate that in the colder section of an engine, such as the compressor, when sand particles are ingested, the biggest issue would most likely be wearing of the compressor blades.

Figure 12 is an optical view of a coupon exposed to pumice under 5x magnification, and Figure 13 is a 3D view of the same coupon at the same magnification.



Figure 12. Optical view of coupon exposed to pumice at 5x magnification

when exposed to particulates for longer periods of time and at higher concentrations, ingestion can lead to significant erosion and damage to the engine [13]. Investigating coupons exposed to higher concentration of pumice and for longer durations could lead to more conclusive results.

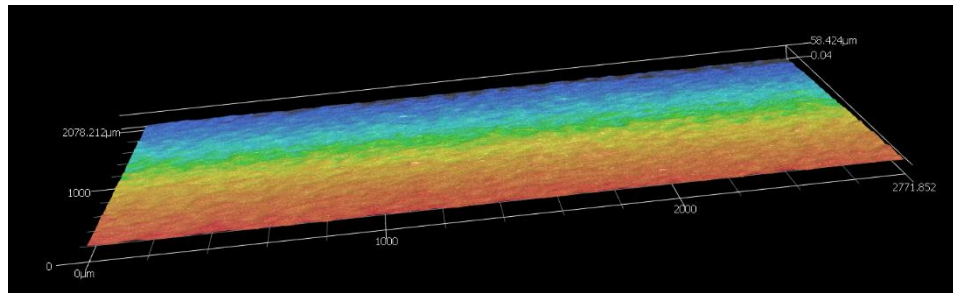


Figure 13. 3D view of coupon exposed to pumice at 5x magnification

Figure 14a, 14b, and 14c show an optical view of a coupon exposed to biochar under 2.5x, 5x, and 10x magnification respectively. Figure 15 shows the same coupon in a 3D view at 5x magnification.

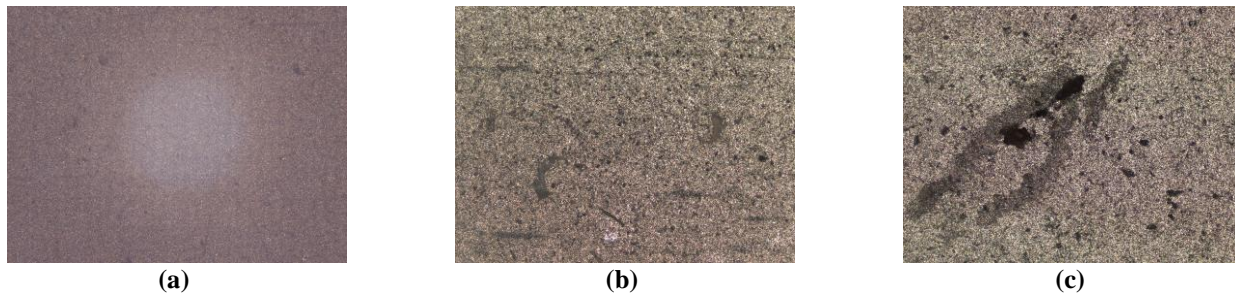


Figure 14. Optical view of coupon exposed to biochar at 2.5x magnification (a) and 5x magnification (b) and 10x magnification (c)

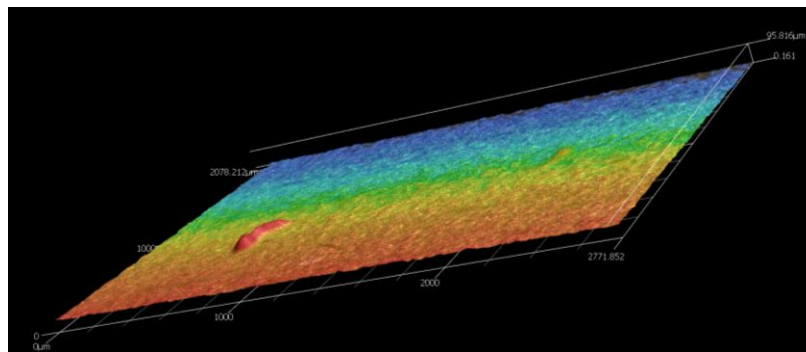


Figure 15. 3D view of coupon exposed to biochar at 5x magnification

In the optical images of the coupons, specifically Figures 14a and b, some of the scratches that were on the coupon initially can still be seen. This signifies that the biochar was not as erosive as the ATD and pumice, which is also consistent with the surface roughness tests. The most notable result that can be seen from the visible inspection is the deposition caused by the biochar. The black spots seen on the coupon, as seen most clearly in Figure 14b and c, are particles of biochar that stuck to the coupon. The 3D scan of the coupon (Figure 15) shows the raised spots of larger places of deposition. These results are consistent with the preliminary testing conducted in 2023. These results suggest that deposition can pose a serious problem for engines exposed to wildfire ash. Even with no added heat, the particles of biochar stuck together and to the surface of the coupon at much higher rates than the other particulates, which suggests that even in the colder sections of the engine, such as the compressor, deposition could occur. Conducting testing with the addition of heat, either to the airflow or the coupons themselves, to simulate the hotter conditions of the engine and environment may show more conclusive results. It is predicted that the hotter temperatures would lead

to an increase in deposition as the particles start to melt. Overall, the visual inspection concluded that the greatest deposition was seen with the biochar, then the ATD, and the least with pumice and confirmed the results found from the surface roughness measurements.

D. Uncertainties and Observations

While this study eliminated the major concerns and sources of uncertainty seen in the preliminary testing, there are still a few sources of uncertainty to note. Firstly, due to the location of the equipment, the coupons had to be transported from the testing location to various labs for analyzation. Each coupon was placed into a small plastic container to minimize exposure to the environment and prevent additional wear. However, even with this measure in place, some of the particulates that were on the coupon were lost in transportation. This could have impacted the results from the visual inspection since some of the particles were knocked off before scanning them with the 3D profilometer. However, if they naturally fell off, it is likely they would have fallen off compressor blades in a real engine and not impacted deposition quantities in the engine.

Another source of uncertainty was the surface roughness measurements. A limitation of the surface roughness tool utilized in this study is that it can only take measurements for a small area of the coupon. To make an accurate comparison of the surface roughness before and after testing, the same area should be measured. Using the tools on hand, a paper was used to mark the place the spot of the surface roughness tool and coupon to attempt to place them in the same spot for each test, however it is unlikely that the same exact spot was measured each time. It is suggested to create a secure set up that holds the surface roughness tool and coupon in place in future experimentation.

Similarly, the 3D profilometer was also limited by a very small field of view, so only a small portion of the coupon could be inspected at a time. This limits the understanding of what is happening at the surface of the entire coupon. Due to time limitations, only a few spots per coupon were investigated. In the future, one solution to this problem is to take multiple images of a coupon and stitch them together to visualize the whole coupon.

There are also potential sources of uncertainty stemming from the particle injection process as not all the particulate material likely hit the coupon. Since there was no procedure used to measure the amount of particulate that hit the coupon vs. went to the side, the following assumptions about the particle distribution were made. To make an accurate comparison between all three particulates, it was assumed that there was an even distribution of the particulates in the free stream and the same area of that distribution hit all the coupons. In other words, the same total amount of particles hit each coupon.

IV. Further Discussion & Conclusions Drawn

An experiment was conducted to measure and compare the erosion and deposition of three particulates (ATD, pumice, and biochar). This study expanded on preliminary research conducted in 2023 by modifying testing procedure to reduce uncertainty and expand the data analysis. The particle refinement process was updated to achieve the desired particle size range, and changes were made to the rig to accommodate more particulates and to fix clogging issues. As a result, tests with a higher flow rate were successfully conducted. To compare the deposition and erosion caused by the three particulates, measurements of the surface roughness and mass were taken. 3D scans and photographs were also taken to visualize differences in the affected coupons. The following conclusions were drawn:

1. Sand had the largest change in surface roughness with an average change of 26.2 micro inches, followed by pumice with an average change of 21.5 micro inches. Biochar saw the smallest change in surface roughness; only an average change of 6.8 micro inches. These measurements indicate that biochar had the least erosive behavior on the coupons compared to the other two particulates.
2. Visual inspection confirmed this result as no scratches were seen on coupons tested with sand and pumice due to erosion, but they were seen on coupons tested with biochar.
3. Biochar resulted in the most deposition, followed by coupons tested with ATD that had some deposition, and coupons tested with pumice saw the least deposition.
4. Mass changes were inconsistent and did not provide useful information. A new method to quantify deposition of particulates will be needed for future studies.
5. The testing procedure and rig set up outlined in this paper can successfully inject biochar into a free stream, confirmed up to 18 g/min with the possibility of higher flow rates.

Pumice exhibited a lower erosion rate than expected due to its porous, lightweight nature and irregular particle shape. These characteristics may have reduced its kinetic energy upon impact with the surface, causing

less abrasion. Additionally, pumice particles could have deformed or shattered rather than scratching the surface, further decreasing the erosion observed.

Biochar showed the highest deposition, likely due to its high porosity and large surface area. These properties allow biochar particles to trap smaller particulates and accumulate more material from the flow, leading to greater deposition on the coupon. Its irregular shape and lower density could also contribute to it settling more easily on the surface.

While mass measurements of deposition were inconsistent, the qualitative observation of increased deposition on biochar was evident through surface texture and roughness changes. The higher deposition may not be reflected in precise mass change, but the visible accumulation and surface changes still suggest biochar's tendency to deposit more material than the other particulates.

V. Future Work

After conducting this study, it is apparent that new measurement techniques are needed to quantify deposition results. Since mass measurements were taken to quantify deposition, but produced inconsistent data, it is recommended to use a different measurement technique. One proposed technique to quantify deposition is to utilize an electron microprobe analyzer. Since the biochar particulates had a much higher deposition level compared to other tested particulates, future research should be conducted to draw new conclusions about the effect of wildfire ash deposition on engines. The successful testing of three different particulates on the rig used in this study indicates this rig may be used in future testing with little uncertainty. Since the rig is now able to handle biochar, this opens the opportunity for many different future studies containing biochar as a particulate.

To build on the findings of this study, one idea for future work is to integrate an electrostatic component into the testing setup. The addition of electrostatics aims to explore how particle charge influences deposition patterns and behaviors on metallic surfaces. Many particulates, including those found in wildfire ash, can carry natural or induced charges, which may significantly alter their interactions with engine components. By incorporating this factor, we hope to better simulate real-world conditions where electrostatic forces can play a role in particulate deposition, particularly within high-temperature and high-flow environments such as those experienced by aviation engines. This enhancement to the rig will allow for controlled testing of charged and neutralized particulates, offering a more comprehensive understanding of deposition mechanisms.

In addition to exploring the role of electrostatics, future experiments could potentially include testing under heated conditions to better replicate the thermal environments experienced by engine components during operation. This might involve heating either the jet flow or the coupons themselves, simulating the high temperatures encountered in real-world scenarios. Heat could significantly influence particulate behavior, particularly in terms of adhesion and chemical interactions with the engine components. Investigating these effects could provide valuable insights into the thermal mechanisms of particulate ingestion.

Another idea to consider is the use of alternating layers of red and blue layout fluid on the coupons to study erosion patterns more effectively. By applying these layers, we could visually inspect and differentiate areas of high deposition and erosion. This approach might offer a clearer understanding of how particulates interact with the surface of the coupon and highlight specific zones of high particulate impact.

Additionally, testing the effects of protective coatings by comparing coated versus uncoated coupons would be an interesting study. Protective coatings, commonly used in aerospace applications, could alter deposition and erosion behavior. Exploring their performance under various particulate interactions may yield insights into their effectiveness in mitigating damage. These findings could potentially inform the selection or development of advanced coatings designed to resist particulate-induced wear.

Acknowledgements

The Wildfire Ash Ingestion Team wishes to acknowledge Pratt & Whitney and Virginia Tech, namely Dr. Charles Haldeman, Dr. Todd Lowe, and Dr. David Gray, for their invaluable guidance and financial support which has made the experiments conducted possible. An additional thanks to past team members Anthony DiGregorio, Michael Walling, and Matthew Morrison for beginning this research and assisting with testing.

References

[1] Hoover, K., and Hanson, L.A., "Wildfire Statistics," 2023.

- [2] Hirschlag, A., "Smoke from burning forests and peat can linger in the atmosphere for weeks, traveling thousands of miles and harming the health of populations living far away." 2020
- [3] Jaynes, H., "Researching the Impact of Fire and Soot on Engine Performance" 2022
- [4] Bojdo, N., Filippone, A., Parkes, B., Clarkson, R., "Aircraft engine dust ingestion following sandstorms." 2020
- [5] Herndon, J., and Whiteside, M., "California Wildfires: Role of Undisclosed Atmospheric Manipulation and Geoengineering" 2018
- [6] Lekki, J., Woike, M., John, C., Venti, M., Mastin, L., "Vehicle Integrated Propulsion Research (VIPR) III Volcanic Ash Ingestion Testing" NASA
- [7] Hsu, K., Barker, B., Varney, B., Boulanger, A., Nguyen, V., Ng, W. (2018). Review of Heated Sand Particle Deposition Models. V02DT47A005. 10.1115/GT2018-75723.
- [8] "U. S. stoneware: Long roll jar mills," *U. S. stoneware* Available: <http://www.usstoneware.com/long-roll-jar-mills.htm>.
- [9] "La-950 Laser Particle Size Analyzer," *HORIBA* Available: <https://www.horiba.com/details/la-950-laser-particle-size-analyzer-108/>.
- [10] "SJ-210 – Portable Surface Roughness Tester," *Mitutoyo* Available: <https://www.mitutoyo.com/products/form-measurement-machine/surface-roughness/sj-210-portable-surface-roughness-tester-2/>.
- [11] "3D surface profiler VK-X3000 series," *KEYENCE* Available: <https://www.keyence.com/products/microscope/laser-microscope/vk-x3000/>.
- [12] "Denver a 200ds dual range balance," *Advanced Test Equipment Corp. - Rentals, Sales, Calibration, Service*. Available: <https://www.atecorp.com/products/denver/a-200ds>.
- [13] Davison, C. R., and Rutke, T. A. (March 13, 2014). "Assessment and Characterization of Volcanic Ash Threat to Gas Turbine Engine Performance." *ASME. J. Eng. Gas Turbines Power*. August 2014; 136(8): 081201. <https://doi.org/10.1115/1.4026810>